Supplementary Materials for

Role of land-ocean interactions in stepwise Northern Hemisphere Glaciation

Yi Zhong *et al*.

Corresponding author: Yi Zhong, zhongy@sustech.edu.cn

Qingsong Liu, qsliu@sustech.edu.cn;

Ning Tan, ning.tan@mail.iggcas.ac.cn

The PDF file includes:
Supplementary Text 1
Supplementary Figures 1 to 8
Supplementary Table 1

Supplementary Text 1. Moisture changes in the dust source regions during the late Pliocene

Environmental changes in the dust source regions play a key role in fueling aeolian dust delivery from the Asian interior. An obvious fundamental turnover in the composition of the desert vegetation in the Qaidam Basin occurred from ~3.6 to 3.3 Myr ago[1]. It is marked by a two- to three-fold increase in *Artemisia* percentages at the expense of other steppe/desert taxa including Ephedraceae, Asteraceae and Tamaricaceae (Fig. 3d). Vegetation turnover events in the Qaidam Basin coincide with the first major expansion of NHIS in the Pliocene[2]. However, a dry climate in desert areas in conjunction with stable land surfaces could potentially lead to higher, lower, or unchanging dust emissions, depending on the overall impact of each part of the system[3]. Therefore, we use the chemical index of alternation (CIA) and Rb/Sr ratios of terrigenous input (Fig. 2e, f) to reconstruct climatic conditions of the source areas. Higher CIA and Rb/Sr ratios suggest enhanced chemical weathering in moister source areas[4,5], while lower CIA and Rb/Sr ratios may indicate the dominance of physical over chemical weathering processes[6]. Application of the CIA proxy necessitates consideration of Na derived from pore water within or passing through the cored sediments. Any non-detrital Na contribution is assumed to be approximately uniform throughout the core. Compared to the relationship between weathering indicators (CIA and Rb/Sr) (Fig. 2e, f) and eolian proxies in ODP Site 1208 (Fig. 3e), enhanced eolian flux is clearly associated with increased chemical weathering in source areas in response to the M2 glacial and iNHG events (Fig. 2d and e). This moisture enhancement in the source area during periods of NHG also shown by the other records from the high and low latitude North Pacific[7,8]. As a result, increased moisture can potentially enhance erosion and weathering, releasing fine particles from parent rocks that are then subject to eolian transportation[9,10,11].

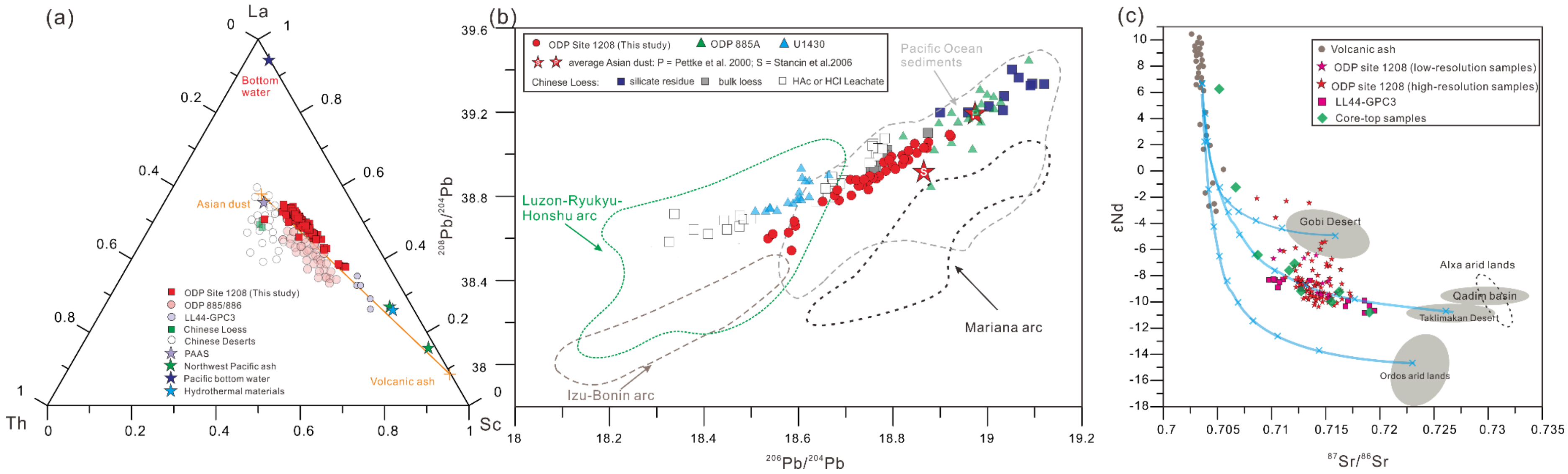

Supplementary Fig. 1. (a) La-Th-Sc diagram. Compositions of northwest Pacific ashes, Pacific bottom waters, and hydrothermal materials are form Bailey[12], Ziegler et al.[13], and Severmann et al.[14], respectively. Also shown are end-members generated by the factor analysis[15]. (b) Pb isotope data for ODP Site 1208 in comparison to other regional archives and input sources. Data source: Pacific Ocean detrital sediments[16,17,18]; volcanic rocks of the lzu-Bonin arc, Mariana arc, and Luzon-Ryuku-Honshu arc; Chinese loess (bulk, residue, and leachates[12, 17, 19]; marine detrital downcore sediments from IODP Site U1340 in the Sea of Japan[20] and ODP Site 885/886 in the North Pacific[21]. Stars represent estimates for the average pre-anthropogenic composition of Asian dust[21,22]. (c) Cross plot between the $^{87}Sr/^{86}Sr$ ratios and εNd values of the operationally defined eolian dust in Pacific sediments[19].

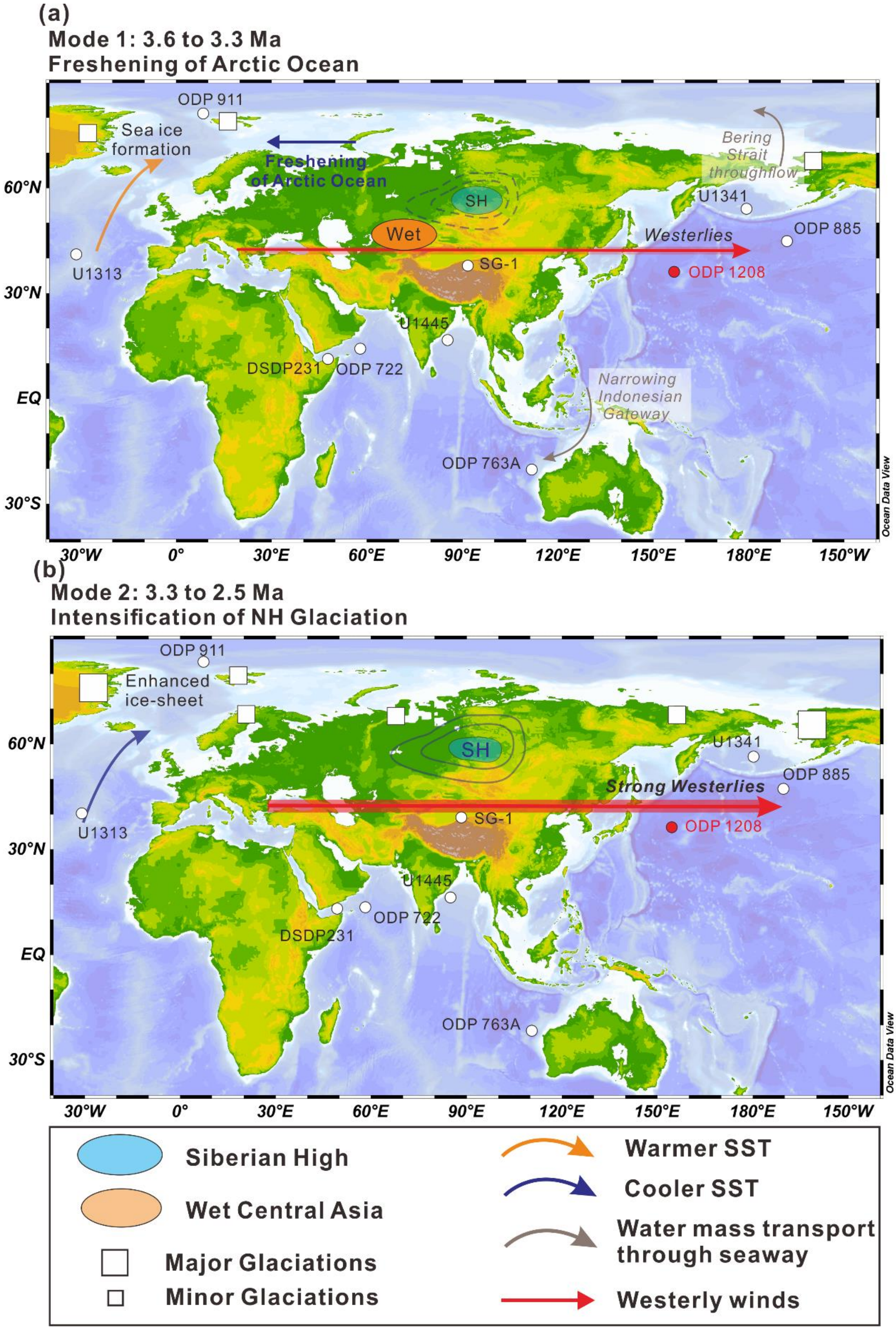

Supplementary Fig. 2. Schematic maps showing stepwise Northern Hemisphere Glaciation and strength of northern hemisphere westerlies from pre- to post-M2 conditions.

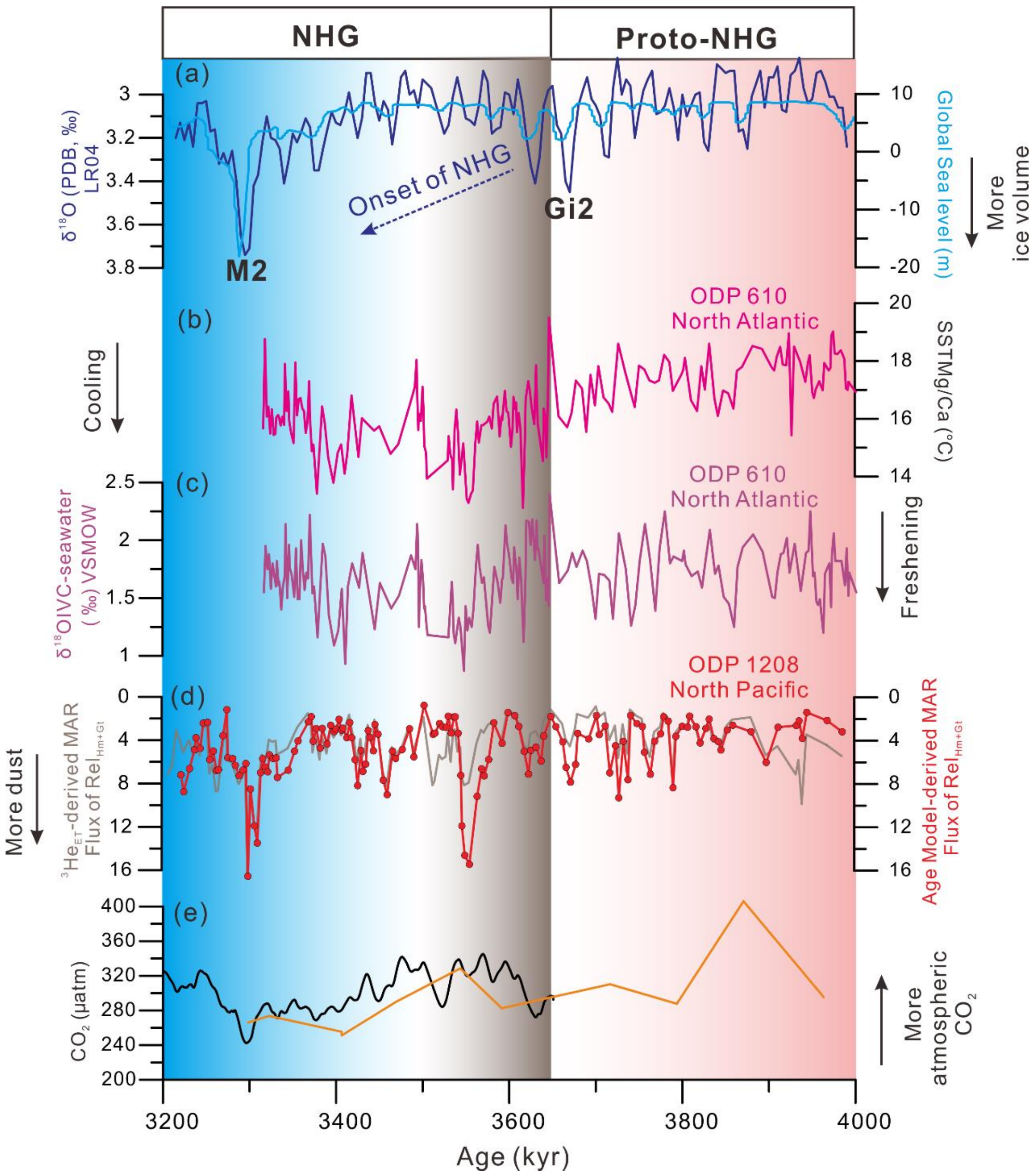

Supplementary Fig. 3. North Pacific dust records and North Atlantic data during the Pliocene. (a) Global benthic $\delta^{18}O$ record[23]; (b) $SST_{Mg/Ca}$ from Site 610A[24]; (c) $\delta^{18}O_{IVC\text{-}seawater}$ values are indicated Pliocene salinities changes[24]; (d) Flux of Rel_{Hm+Gt} and based on age (red) and ^{3}He[25] (grey) for ODP Site 1208; (e) Atmospheric pCO_2 based on planktonic foraminifera $\delta^{11}B$[26] (yellow) and model simulations[27] (black).

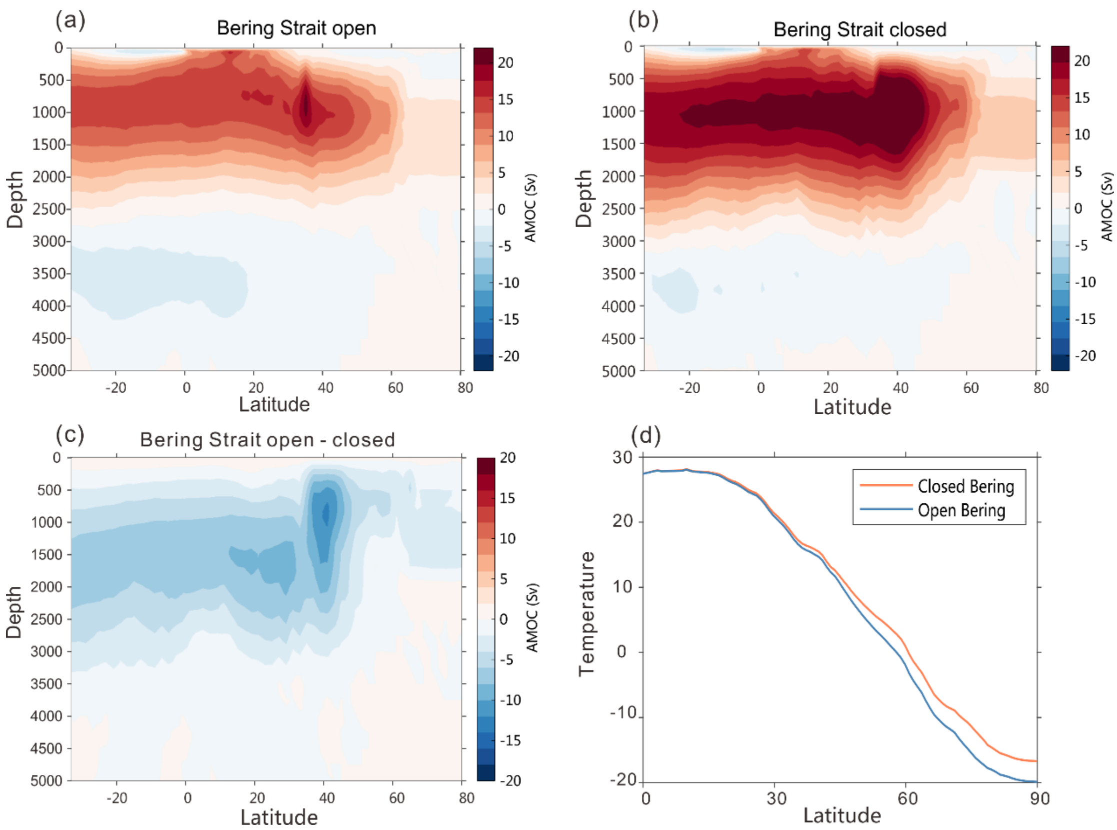

Supplementary Fig. 4. Climate response to a closed Bering Strait simulated by the Community Climate System Model, version 4 (CCSM4). a) Atlantic Meridional Overturning Circulation (AMOC) in an open Bering Strait (BS) scenario. b) AMOC in a closed BS scenario. c) The difference in AMOC strength between the open BS and closed BS scenarios. d) zonal mean surface air temperature in the Northern Hemisphere in the open BS (blue) and closed BS (orange) scenarios, showing a steeper meridional temperature gradient due to reduce northward heat transport driven by a weaker AMOC in the open BS scenario.

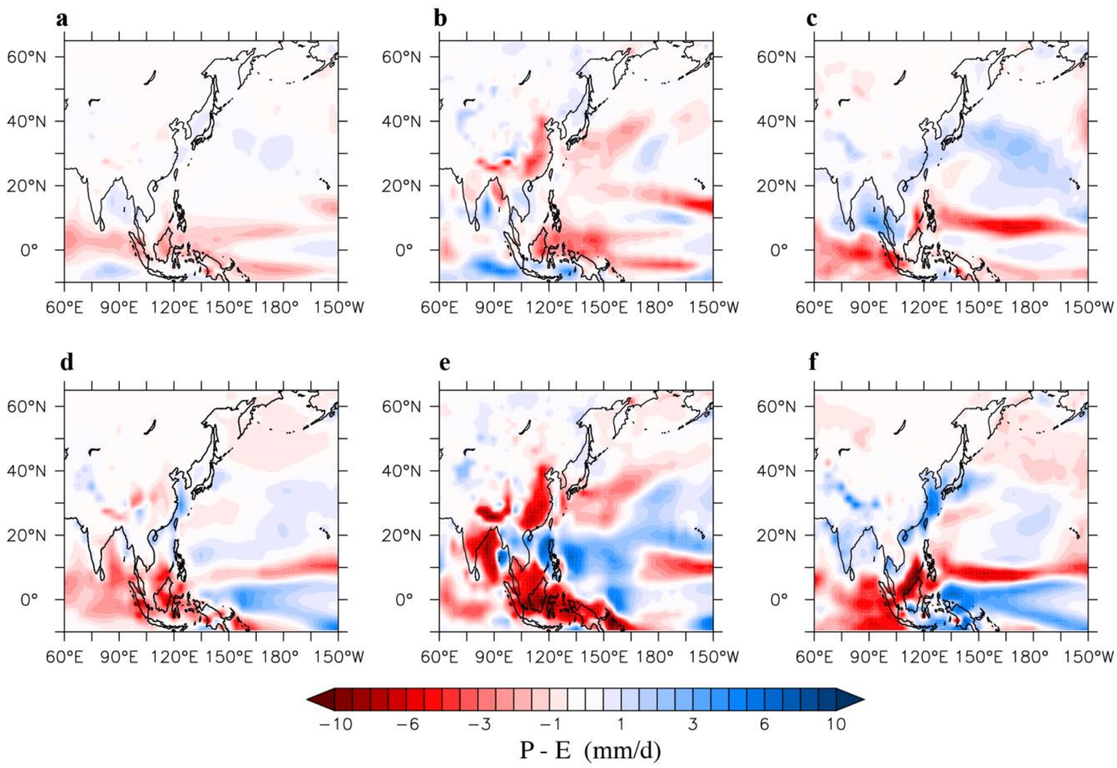

Supplementary Fig. 5. Changes in precipitation minus evaporation when compared to the warm mPWP (PlioMIP 1). The upper panel shows results for MIS M2, while the bottom panel shows results for iNHG. Panels a/d, b/e, c/f represent the annual mean, summer and winter results, respectively. Overall, aridification occurred during glacials compared to mPWP during the Pliocene.

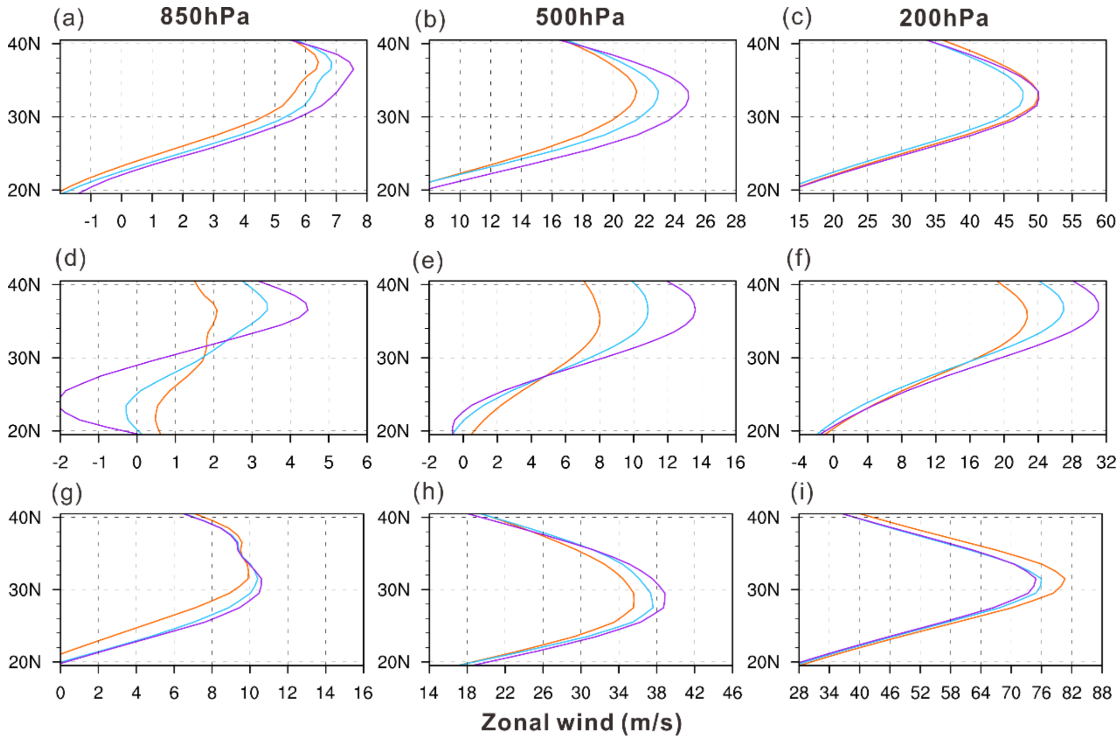

Supplementary Fig. 6. Zonal wind at different pressure levels. The average zonal wind is the same as in the Figure. 5. It is calculated for longitudes between 120 °E and 150 °E, corresponding to the dominant dust source region in the North Pacific. The orange, blue and purple curves represent PlioMIP1, MIS M2 and iNHG simulations, respectively. The subplots (a, b, c) / (d, e, f) / (g, h, i) represent the mean annual, summer and winter results, respectively.

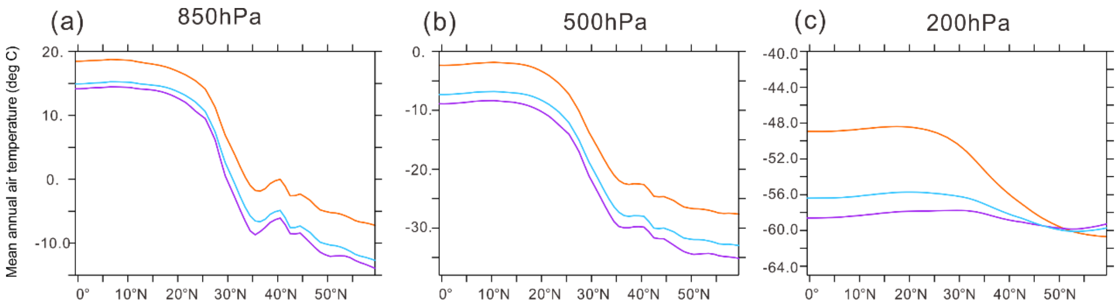

Supplementary Figure 7. The distribution of zonal mean temperature at different altitudes over the Eurasian region (0 °N-60 °N, 70 °E-150 °E) during PlioMIP 1 (orange line), MIS M2 (blue line), and iNHG (purple line).

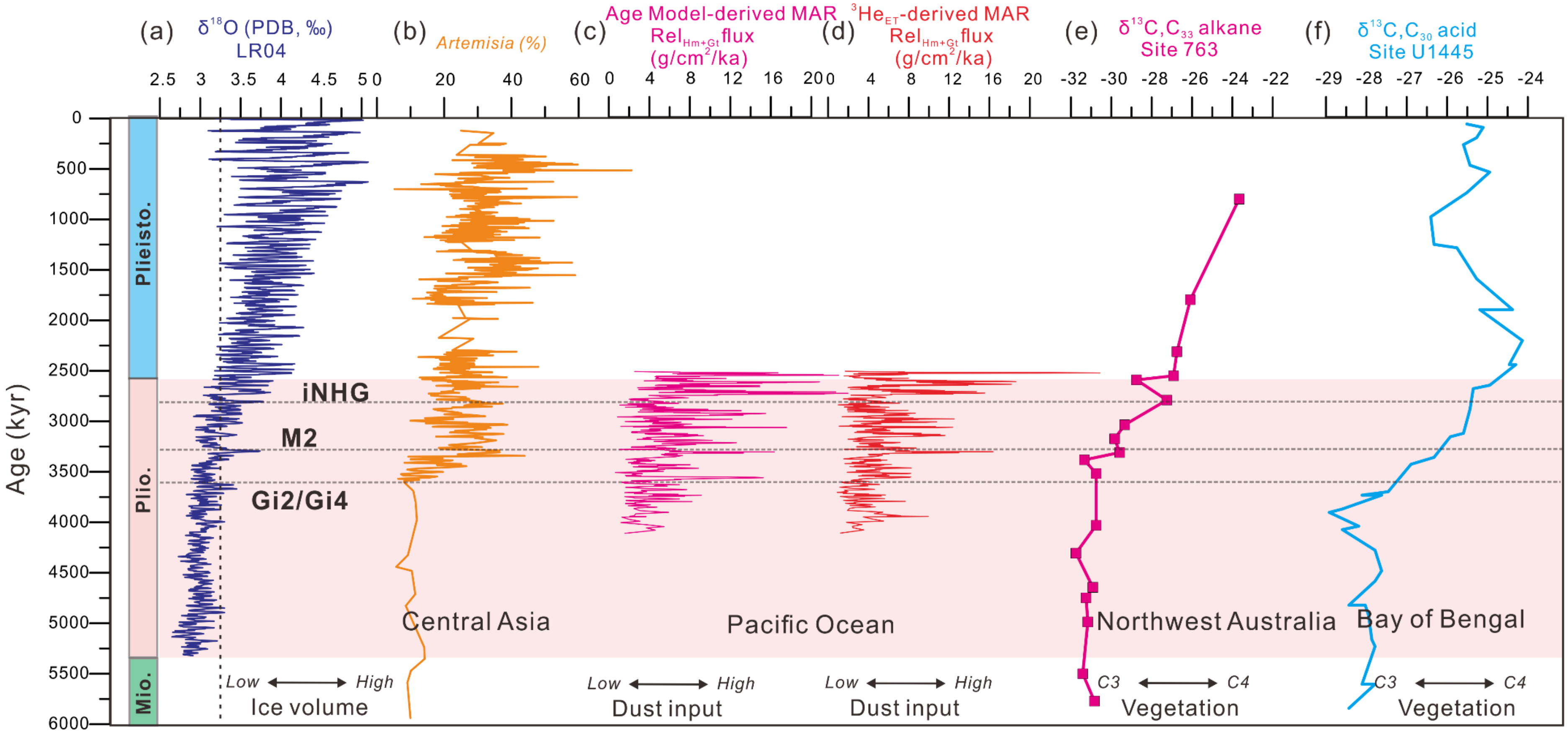

Supplementary Fig. 8. ODP Site 1208 dust records in the context of global terrestrial plant changes (a) Global benthic $\delta^{18}O$ record[23]; (b) *Artemisia* pollen percentages at site SG-1 from the Qaidam Basin[1]; (c) Flux of Rel_{Hm+Gt} for ODP 1208 (this study); (d) Flux of Rel_{Hm+Gt} calculated from ^{3}He-derived MAR[25] for ODP Site 1208 (this study); (e) $\delta^{13}C$ of C_{33}-alkanes from northwest Australia[28]; (f) $\delta^{13}C$ of C_{30}-fatty acid at Site U1445 from the Bay of Bengal, which reflects vegetation type changes from the Mahandi basin on the Indian Peninsula[29].

Supplementary Table 1. The mean, median and standard deviations of Rel_{Hm+Gt} fluxes over four time windows ODP 1208.

	Age Model-derived Rel_{Hm+Gt} Fluxes			$^3He_{ET}$-derived Rel_{Hm+Gt} Fluxes		
Time Interval	**Mean**	**Median**	**Standard Deviation**	**Mean**	**Median**	**Standard Deviation**
2.5-2.73 Ma	10.22	8.38	5.55	8.06	6.89	5.41
2.73-3.31 Ma	5.75	5.38	2.89	5.20	4.58	2.75
3.31-3.55 Ma	5.18	5.17	2.98	4.45	4.22	1.69
3.55-4.1 Ma	3.97	3.54	2.08	3.32	2.92	1.74

Supplementary References

1. Koutsodendris, et al. Late Pliocene vegetation turnover on the NE Tibetan Plateau (Central Asia) triggered by early Northern Hemisphere glaciation. *Global and Planetary Chang*e **180**, 117–125 (2019).

2. De Schepper, S., Gibbard, P.L., Salzmann, U., & Ehlers, J. A global synthesis of the marine and terrestrial evidence for glaciation during the Pliocene Epoch. *Earth-Science Reviews* **135**, 83–102 (2014).

3. Pye, K. Processes of Fine Particle Formation, Dust Source Regions, and Climatic Changes, in: Leinen, M., Sarnthein, M. (Eds.), Paleoclimatology and Paleometeorology: Modern and Past Patterns of Global Atmospheric Transport. Springer Netherlands, Dordrecht, pp. 3–30 (1989).

4. Chen, J., An, Z., & Head, J. Variation of Rb/Sr ratios in the loess-paleosol sequences of central China during the last 130,000 years and their implications for monsoon paleoclimatology. *Quaternary Research* **51**, 215-219 (1999).

5. Dasch, E. J. Strontium isotopes in weathering profiles, deep-sea sediments, and sedimentary rocks. *Geochimica et Cosmochimica Acta* **33**, 1521-1552 (1969).

6. Fedo, C. M., Wayne Nesbitt, H., & Young, G. M. Unraveling the effects of potassium metasomatism in sedimentary rocks and paleosols, with implications for paleoweathering conditions and provenance. *Geology* **23**, 921-924 (1995).

7. Zhang, Q. et al. Mechanism for enhanced eolian dust flux recorded in North Pacific Ocean sediments since 4.0 Ma: Aridity or humidity at dust source areas in the Asian

interior? *Geology* **48**, 77–81 (2020).

8. Zhong, Y., et al. Humidification of Central Asia and equatorward shifts of westerly winds since the late Pliocene. *Communications Earth & Environment* **3**, 274 (2022).

9. Kocurek, G., & Lancaster, N. Aeolian system sediment state: theory and Mojave Desert Kelso dune field example. *Sedimentology* **46**, 505-515 (1999).

10. Nie, J., Pullen, A., Garzione, C. N., Peng, W., & Wang, Z. Pre-Quaternary decoupling between Asian aridification and high dust accumulation rates. *Science Advances* **4**, eaao6977 (2018).

11. Nie, J. et al. Loess Plateau storage of Northeastern Tibetan Plateau-derived Yellow River sediment. *Nature Communications* **6**, 8511 (2015).

12. Bailey, J. C. Geochemical history of sediments in the northwestern Pacific Ocean. *Geochemical Journal*, **27**(2), 71–90 (1993).

13. Ziegler, C. L., Murray, R. W., Hovan, S. A., & Rea, D. K. Resolving eolian, volcanogenic, and authigenic components in pelagic sediments from the Pacific Ocean. *Earth and Planetary Science Letters*, **254**(3), 416–432 (2007).

14. Scheinost, A. C., Chavernas, A., Barrón, V., & Torren, J. Use and limitations of second-derivative diffuse reflectance spectroscopy in the visible to near-infrared range to identify and quantify Fe oxide minerals in soils. *Clays and Clay Minerals*, **46**, 528–536 (1998) https://doi.org/10.1346/CCMN.1998.0460506.

15. Zhang, W., Chen, J., Ji, J., & Li, G. Evolving flux of Asian dust in the North Pacific Ocean since the late Oligocene. *Aeolian Research* **23**, 11–20 (2016).

16. Godfrey, L. V. Temporal changes in the lead isotopic composition of red clays: comparison with ferromanganese crust records. *Chem. Geol.* **185**, 241–254 (2002).

17. Jones, C. E., Halliday, A. N., Rea, D. K. & Owen, R. M. Eolian inputs of lead to the North Pacific. *Geochim. Cosmochim. Acta.* **64**, 1405–1416 (2000).

18. Pettke, T., Halliday, A. N. & Rea, D. K. Cenozoic evolution of Asian climate and sources of Pacific seawater Pb and Nd derived from eolian dust of sediment core LL44-GPC3. *Paleoceanography* **17**, PA000673 (2002).

19. Ling, H. F. et al. Differing controls over the Cenozoic Pb and Nd isotope evolution of deepwater in the central North Pacific Ocean. *Earth Plant. Sci. Lett.* **232**, 345–361 (2005).

20. Shen et al. History of Asian eolian input to the Sea of Japan since 15 Ma: Links to Tibetan uplift or global cooling? *Earth Planet. Sci. Lett.* **474**, 296–308 (2017).

21. Pettke, T., Halliday, A. N. & Rea, D. K. Cenozoic evolution of Asian climate and sources of Pacific seawater Pb and Nd derived from eolian dust of sediment core LL44-GPC3. *Paleoceanography* **17**, PA000673 (2002).

22. Stancin, A. M. et al. Radiogenic isotopic mapping of late Cenozoic eolian and hemipelagic sediment distribution in the east-central Pacific. Earth Planet. Sci. Lett. 248, 840–850 (2006).

23. Lisiecki, L. E., & Raymo, M. E. A Pliocene-Pleistocene stack of 57 globally distributed benthic $\delta^{18}O$ records. *Paleoceanography* **20**, PA1003 (2005).

24. Knies, J., et al. Effect of early Pliocene uplift on late Pliocene cooling in the Arctic–Atlantic gateway. *Earth and Planetary Science Letters* **387**, 132–144 (2014).

25. Abell, J. T., Winckler, G., Anderson, R. F., & Herbert, T. D. Poleward and weakened westerlies during Pliocene warmth. *Nature* **589**, 70–75 (2021).

26. Rae, J. W. B. et al. Atmospheric CO_2 over the Past 66 Million Years from Marine Archives. *Annual Review of Earth and Planetary Sciences* **49**, 609–641 (2020).

27. Dowsett, H. J. et al. Assessing confidence in Pliocene sea surface temperatures to evaluate predictive models. *Nature Climate Change* **2**, 365–371 (2012).

28. Andrae, J. W. et al. Initial Expansion of C4 Vegetation in Australia During the Late Pliocene. *Geophysical Research Letters* **45**, 4831–4840 (2018).

29. Dunlea, A. G., Giosan, L., & Huang, Y. Pliocene expansion of C4 vegetation in the core monsoon zone on the Indian Peninsula. Clim. Past Discuss. 2020, 1–17.